

pubs.acs.org/est Article

# Electrosorption Integrated with Bipolar Membrane Water Dissociation: A Coupled Approach to Chemical-free Boron Removal

Sohum K. Patel, Weiyi Pan, Yong-Uk Shin, Jovan Kamcev, and Menachem Elimelech\*



Cite This: Environ. Sci. Technol. 2023, 57, 4578–4590



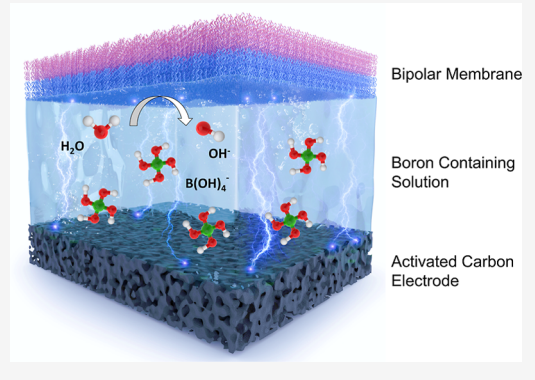
**ACCESS** 

III Metrics & More

Article Recommendations

s Supporting Information

ABSTRACT: Boron removal from aqueous solutions has long persisted as a technological challenge, accounting for a disproportionately large fraction of the chemical and energy usage in seawater desalination and other industrial processes like lithium recovery. Here, we introduce a novel electrosorption-based boron removal technology with the capability to overcome the limitations of current state-of-the-art methods. Specifically, we incorporate a bipolar membrane (BPM) between a pair of porous carbon electrodes, demonstrating a synergized BPM—electrosorption process for the first time. The ion transport and charge transfer mechanisms of the BPM—electrosorption system are thoroughly investigated, confirming that water dissociation in the BPM is highly coupled with electrosorption of anions at the anode. We then demonstrate effective boron removal by the BPM—electrosorption system and verify that the mechanism for boron removal is electrosorption, as opposed to adsorption on



the carbon electrodes or in the BPM. The effect of applied voltage on the boron removal performance is then evaluated, revealing that applied potentials above  $\sim 1.0$  V result in a decline in process efficiency due to the increased prevalence of detrimental Faradaic reactions at the anode. The BPM-electrosorption system is then directly compared with flow-through electrosorption, highlighting key advantages of the process with regard to boron sorption capacity and energy consumption. Overall, the BPM-electrosorption shows promising boron removal capability, with a sorption capacity >4.5  $\mu$ mol g-C<sup>-1</sup> and a corresponding specific energy consumption of <2.5 kWh g-B<sup>-1</sup>.

KEYWORDS: bipolar membrane, boron, electrochemistry, desalination, electrosorption, electrified water treatment, chemical free, post-treatment

#### ■ INTRODUCTION

Boron is ubiquitous in seawater, typically ranging in concentration from 4 to 6 mg L<sup>-1</sup>. Although an essential micronutrient, excess boron intake is highly toxic to humans and many crops, making effective boron removal in seawater desalination critical. Additionally, boron removal is necessary for the treatment of many contaminated groundwaters (e.g., several well water sources in California)1,2 and in the production of ultrapure water (e.g., for the microelectronics and semiconductor industries).3 Boron is also a detrimental contaminant in battery-grade lithium carbonate, requiring its effective extraction during lithium recovery and refining.<sup>4,5</sup> Reverse osmosis (RO), the most widely utilized technology for solute-water separation, rejects species based on the combined effects of size and charge, rendering boron—present in natural waters as the small and uncharged boric acid molecule—a particularly difficult contaminant to remove.<sup>6</sup> Hence, the typical rejection of boron by RO membranes (<80%) is insufficient, requiring the use of chemical, energy, and capital-intensive post-treatment processes to reduce boron concentrations to permissible levels.

The removal of trace levels of boron from aqueous solutions has proven to be a challenging task, culminating in only a few effective boron separation methods to date. Specifically, multipass high pH RO and boron-selective sorbents are the most cost effective and practical methods. The use of multipass RO—in which the permeate from an initial RO pass is repressurized, dosed with base (to convert the boric acid to the borate anion), and sent through another pass (or several additional passes) RO—is the most commonly employed method for achieving high degrees of boron removal. The inherent pH swings of the process require substantial chemical dosing, which is uneconomical and environmentally unsustainable. The additional RO passes also increase the overall energy consumption of the seawater desalination process by an estimated 10–15%.

Received: January 5, 2023 Revised: February 22, 2023 Accepted: February 23, 2023 Published: March 9, 2023





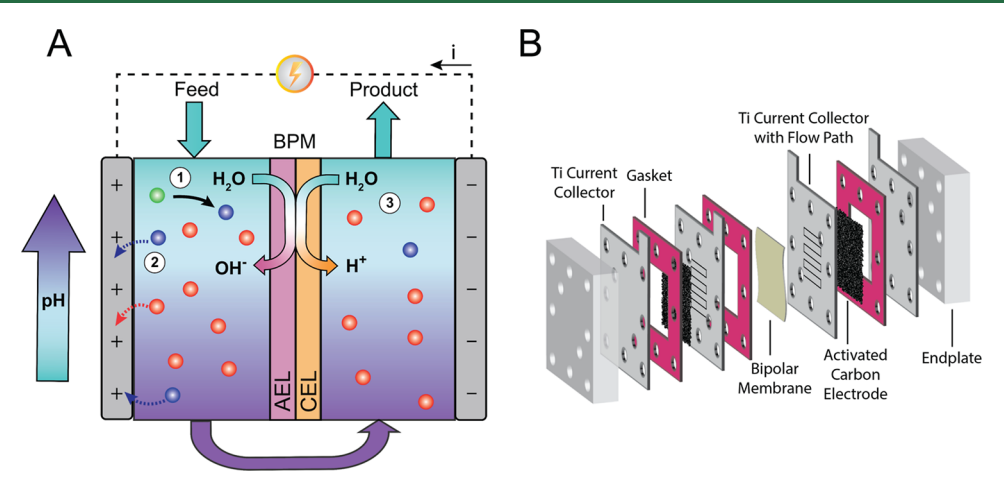


Figure 1. (A) Process schematic of BPM-electrosorption for boron removal. A BPM is placed between a pair of activated carbon electrodes, resulting in two separate flow channels. When a sufficient potential is applied across the BPM, water dissociates to produce hydroxides on the anode side and protons on the cathode side. Boron-contaminated water is fed to the anode side, where the boric acid (green sphere) is converted to borate anion (blue spheres) and subsequently electrosorbed at the anode. Additional anionic species (e.g., chloride) may also be electrosorbed and are depicted by the red spheres. The high-pH, boron-depleted effluent from the anode compartment may then be directed into the cathode side, where the protons produced by the BPM neutralize the pH, generating the final boron-free product water. Upon saturation of the electrodes, the cell is short circuited (or the polarity is reversed) to release the electrosorbed ions into a boron-rich brine stream. (B) Illustration of the constructed BPM-electrosorption device and its individual components. The device consists of activated carbon cloth electrodes, a BPM, two flow paths, and titanium current collectors.

Adsorption of boron using chelating resins is the typical alternative to the multi-pass RO scheme. Although many commercial resins have demonstrated highly effective boron removal in full-scale continuous flow operation, <sup>13–16</sup> relatively slow removal kinetics necessitate large and costly bed volumes. The repeated swelling and shrinking of the polymeric resins, brought on by sorbent regeneration cycles, accelerate the deterioration of adsorption capacity, thereby limiting the effective lifecycle of the resins. <sup>13</sup> Furthermore, the regeneration of the resins also uses large quantities of strong acids or bases as eluting agents, incurring greater financial and environmental costs. <sup>8,13,14</sup> The major shortcomings of both multi-pass RO and boron-selective sorbents warrant the investigation of a new and improved boron removal technology.

A process which has gained considerable attention in the past decade for water deionization is electrosorption. <sup>17–19</sup> In electric double layer-based electrosorption, a small electric potential (<1.4 V) is applied between a pair of porous carbonbased electrodes. The applied voltage generates an electric field, driving ions in solution into the oppositely charged electrode, where they are immobilized in the electrical double layers (EDLs) of the micropores. With the extremely high surface areas of porous carbon materials (i.e,  $>1000 \text{ m}^2 \text{ g}^{-1}$ ), <sup>17</sup> a considerable amount of ions can be removed from solution prior to electrode saturation. When the electric potential is removed or reversed, the ions are released from the EDLs back into the solution, producing a brine stream and regenerating the electrode sorption sites.<sup>19</sup> Electrosorption performs most efficiently for low salinity waters and small extents of ion removal; 20,21 hence, its use for trace boron removal (e.g., from seawater RO permeate) is expected to be an energetically favorable application of the technology which, aside from a few recently proposed schemes, 22,23 remains largely unexplored. For the electrosorption of boron at the anode, however, boric acid  $(pK_a \sim 9.1)^{24}$  must be ionized to borate under high pH conditions. Opportunely, with electrosorption being an electrically driven process, unlike conventional boron removal

methods, it is possible to circumvent reliance on chemical dosing for the necessary pH adjustment.

A method which offers reliable, energy efficient, and tunable electrochemical pH control is bipolar membrane (BPM)induced water dissociation. BPMs, a distinctive type of ionexchange membrane, consist of an anion exchange layer (AEL) (i.e., selective for anion permeation) and a cation exchange layer (i.e., selective for cation permeation) laminated together.<sup>25</sup> Hence, whereas conventional ion-exchange membranes are used for the selective transport of either cations or anions, BPMs ideally restrict the transport of all ions across the membrane. Thus, when the BPM is oriented with the AEL facing the anode and the cation exchange layer facing the cathode (i.e., reverse bias operation) and a sufficient potential difference is applied, the lack of transmembrane charge carriers is compensated by the dissociation of water molecules at the membrane's interfacial junction, in turn generating hydroxide ions and protons on opposite sides of the membrane to sustain the flow of current. $^{26-28}$  It is important to note that BPMcatalyzed water dissociation is distinct from water electrolysis, with the latter referring to the water splitting electrode surface reactions that result in gas evolution and a local acidic pH at the anode. In contrast, BPM water dissociation produces no gaseous byproducts, requires a lower operating voltage (i.e., lower theoretical energy consumption per amount of acid/base generated), and is achieved with the AEL facing the anode, generating a high anodic pH-as is required for boron electrosorption.<sup>29</sup> Historically, BPMs have been primarily applied to electrodialysis processes to generate acid and base products.<sup>28</sup> The integration of BPMs into capacitive electrode processes, however, is largely unfamiliar and presents a unique platform for the direct removal and potential recovery of weak acid and base species, such as boron.

In this study, we demonstrate a proof of concept for a novel electrochemical process (Figure 1A), which implements the use of a BPM between a pair of porous carbon electrodes to couple precise electrochemical pH control with electrosorption of boron. We begin by investigating the underlying transport

and reaction mechanisms unique to the BPM—electrosorption system, identifying both the favorable and parasitic phenomena toward the overall process efficiency. Upon introducing boron to the feedwater, we demonstrate successful boron removal and desorption and further validate that the boron removal mechanism is indeed electrosorption. After confirming successful boron electrosorption, we investigate the effects of process conditions, uncovering tradeoffs and opportunities for performance optimization with respect to the applied voltage. We conclude by highlighting the key advantages of the BPM-electrosorption technology for boron removal.

#### ■ MATERIALS AND METHODS

**Materials and Chemicals.** Granular boric acid (J.T. Baker, >99.5%), sodium chloride (Sigma-Aldrich, >99%), and sodium bromide (Sigma-Aldrich, >99.5%) were dissolved in Milli-Q ultrapure deionized water (>18  $M\Omega$ ) for the preparation of various feedwater solutions. Ultrapure carrier grade compressed nitrogen was obtained from Airgas and used for purging feed solutions.

An ultra-corrosion-resistant grade 2 titanium sheet (0.02 in. thickness, McMaster Carr) was used for the current collectors, and acrylic plates (0.5 in. thickness, McMaster Carr) were used for the endplates. Ultra-thin silicone (0.01 in. thickness, McMaster Carr) was utilized for the membrane gasket material, while a slightly thicker (0.03 in. thickness, McMaster Carr) water and steam-resistant EPDM rubber was used for the gaskets that house the electrodes.

Commercially available knitted activated carbon cloth (CarboCloth, Charcoal House) was used as the electrode material for both the anode and cathode. The Brunauer–Emmet–Teller (BET) surface area of the carbon cloth material was measured as 1001.6 m² g⁻¹. The pore size distribution was determined using Barrett–Joyner–Halenda analysis, revealing that the carbon cloth has a highly microporous structure, with the majority of pores being <2 nm in diameter (Figure S1). A commercially available BPM (Fumasep FBM with PEEK reinforcement, Fuel Cell Store) was utilized throughout the study.

**Electrochemical Cell Design.** The BPM-electrosorption cell consists of several components, as illustrated in Figure 1B. Specifically, two  $(2 \text{ in.} \times 2 \text{ in.})$  activated carbon cloth electrodes  $(185 \pm 9 \text{ mg} \text{ each})$  are separated by a  $(2 \text{ in.} \times 2 \text{ in.})$  BPM placed between two  $(9.0 \text{ cm}^2)$  serpentine flow paths. The cell is sealed with rubber gaskets between the electrodes and the membrane, and all the components are compressed into a stack using acrylic endplates and glass-reinforced nylon screws. The flow paths and holes were precisely cut into each of the materials using a CNC milling machine.

We orient the etched titanium current collectors between the electrodes and BPM to allow the solution to effectively make contact with both the BPM and electrodes. Furthermore, the placement of the etched current collectors effectively connects the BPM and electrodes electrically in parallel, circumventing the otherwise large potential drop across the BPM and ensuring the same potential difference both across the BPM and across the electrodes. We also add additional titanium current collectors (without a flow path) to the adjacent side of each electrode to maximize contact of the electrode with current collectors, in effect minimizing the contact resistance.

**Performance Testing.** The electrochemical flow cells were either operated in single-pass or batch mode. In single pass

mode (Figure S3), feedwater, consisting of 5 mM NaCl and 1 mM B(OH)<sub>3</sub> (unless otherwise specified), was pumped from a 20 L polypropylene reservoir to the cell using a MasterFlex L/S peristaltic pump at a flowrate of 1.0 mL min<sup>-1</sup>. The pH, conductivity, and dissolved oxygen (DO) of the effluent from the anode side were continuously measured and recorded in 20 s intervals using in-line probes inserted into a custom-made acrylic probe holder with a cylindrical flow path. Time series effluent samples were collected by opening an in-line four-way stop-cock for 30 s (0.5 mL samples). Prior to applying a potential, solution was pumped from the feed reservoir through the cell overnight to ensure both the membrane and electrodes were fully equilibrated with the feed solution. Samples were collected from three consecutive cycles which followed three initial conditioning charge-discharge cycles. Additionally, to more clearly investigate the mechanisms of the BPM-electrosorption process, DO was removed from the solution prior to feeding the electrosorption device. Specifically, the feed reservoir, which was equipped with a pressure relief valve, was thoroughly sparged with nitrogen gas until the DO concentration in the anode-side effluent was below 0.5 mg  $L^{-1}$ .

In batch mode experiments (Figure S4), two separate feed reservoirs, each consisting of the same 25.0 mL of feed solution (5 mM NaBr), were recirculated through adjacent sides of the cell at 3.0 mL min<sup>-1</sup>. The solutions were sealed off from the atmosphere and sparged with wet nitrogen to remove DO. A nitrogen blanket was continuously maintained in the headspace of each solution to prevent the dissolution of atmospheric gases. A pH probe was inserted into each feed reservoir to continuously monitor changes in pH. The solutions were circulated through the cell for 2 h prior to beginning the experiments to ensure equilibration with the membranes and the electrode, thereby minimizing the effects of adsorption. Samples (0.15 mL) were collected using a permanently inserted syringe needle to avoid exposure of the solution to the atmosphere during sample collection. Like in single pass mode, all sampling was completed after three charge-discharge cycles to ensure the system had achieved a dynamic equilibrium, and three consecutive cycles were tested to obtain triplicate data.

To elucidate the mechanisms of the investigated process and reduce system complexity, the same feedwater was fed to the anode and cathode chambers separately. We note, however, that a more practical operation mode of the process would be to feed the effluent from the anode side into the cathode side flow channel, resulting in a circumneutral pH of the final boron-depleted product water (from the cathode chamber), as illustrated in Figure 1A. Although not directly demonstrated in this study, such an operation mode will be investigated in our future work.

A CH Instruments 600E potentiostat was used to regulate the applied potential throughout the experiments, with the current being recorded in 1 s intervals. The boron concentration of the collected samples was measured using a PerkinElmer Nexion 5000 Multi-Quadrapole inductively coupled plasma mass spectrometer (ICP–MS). Sodium, bromide, and chloride concentrations were obtained using a Metrohm 940 Professional IC Vario ion chromatograph. All samples were collected and stored in polypropylene containers to avoid potential contamination from borosilicate glassware.

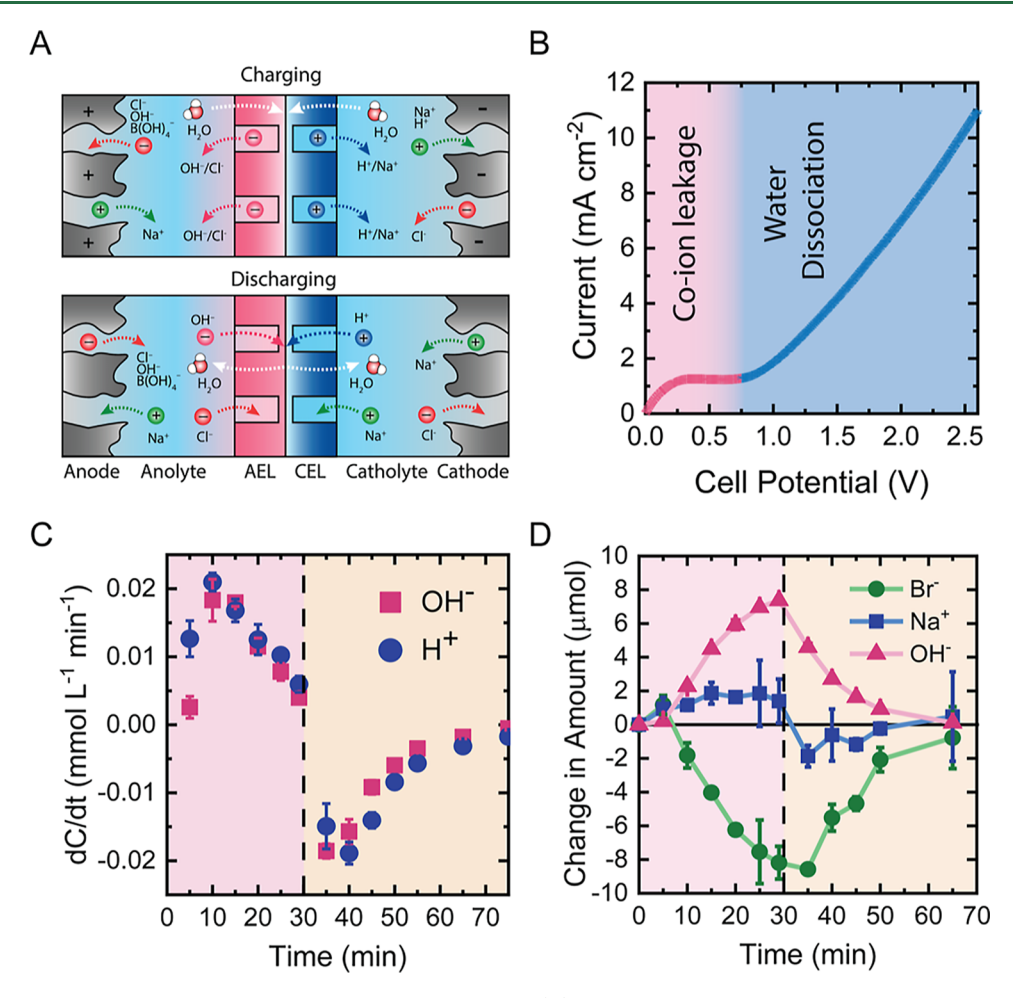


**Figure 2.** Evaluation of mechanisms in the BPM-electrosorption system. (A) Schematic illustration of the theorized charging and discharging mechanisms in the BPM-electrosorption system. (B) Change in BPM-electrosorption process mechanisms as a function of applied cell voltage. The regimes are identified according to the response in current as the voltage is linearly swept at a 5 mV s<sup>-1</sup> scan rate. The flow cell was operated in a single pass configuration with 500 mM NaCl feedwater to clearly identify characteristic features of BPM water dissociation. (C) Change in the hydroxide and proton concentrations with respect to time in the anolyte and catholyte solutions, respectively. Experiments were conducted in batch recirculation mode with 5 mM NaBr anolyte and catholyte solutions under 1.4 V for charging and 0 V for discharging. (D) Complete species balances for the anolyte solution over time for 5 mM NaBr batch experiments. The change in the amount of each species with respect to the initial concentration (i.e., before applying a potential) is shown, with negative and positive values indicating the removal and addition of the species from the recirculating batch solution, respectively. In both (C,D), the charging duration is shown in the pink background, while the discharging duration is represented by the orange background.

#### ■ RESULTS AND DISCUSSION

### Validation of BPM-Electrosorption Mechanisms.

Because BPM-assisted electrosorption is a novel concept to the literature, we begin by proposing and validating the underlying process mechanisms during the charging and discharging phases of operation. It is important to note that the inclusion of a BPM and the use of two flow channels fundamentally alter the conventional electrosorption (CDI) process, which consists of only a single flow channel between a pair of capacitive electrodes. Specifically, with two separate flow channels, charge neutrality must be maintained in each solution independently throughout the deionization and electrode regeneration periods. In typical ion-exchange membrane processes, which use multiple flow channels between electrodes (e.g., water electrolysis, electrodialysis, fuel cells, and redox flow batteries), charge neutrality is ensured in each channel through the transport of ions across the ion exchange membranes. 30 However, BPMs ideally restrict the passage of all ions across the membrane, with practical

membranes only allowing a small leakage of co-ions through.<sup>26</sup> Thus, at relatively high currents in the BPM-electrosorption process, charge neutrality in the flow channels must be maintained through the direct coupling of the electrode and BPM processes, as depicted in Figure 2A.

The mechanistic illustration in Figure 2A, provided for the case of a boron-containing sodium chloride feed solution, shows the hypothesized ion transport mechanisms for both the charging and discharging steps. In the charging step, the membrane is under reverse bias operation (i.e., the AEL faces the anode, and the CEL faces the cathode), inducing water dissociation at the interfacial junction after the membrane has been depleted of priorly stored mobile charge carriers (i.e., predominantly chloride in the AEL and sodium in the CEL). As hydroxides and protons are produced from water dissociation, they are transported into adjacent flow channels through the AEL and CEL, respectively. To satisfy the condition of charge neutrality in the anolyte, the release of a hydroxide ion from the BPM (or a chloride ion during initial membrane ion depletion) must be accompanied by the

simultaneous electrosorption of an anion (i.e., chloride, borate, or hydroxide ion) or co-ion expulsion of a cation (i.e., sodium ion) from the electrode. Similarly, each proton contributed to the catholyte (from BPM water dissociation) must be paired with the electrosorption of a sodium ion or proton or the co-ion expulsion of a chloride ion. Borate is not considered as a relevant ion for co-ion expulsion (from the cathode), as the pH of the catholyte is expected to remain below the  $pK_a$  of boric acid. It should be noted that co-ion expulsion, like in conventional electrosorption processes, is parasitic toward current efficiency and should ideally be minimized.

For the discharging process, we consider the case of short circuiting the electrodes (i.e., 0 V). During discharging, the ions previously electrosorbed in the electrodes are released back into each flow channel. However, because the flow channels are separated by the BPM, the rate of ion release is coupled to that of water reformation in the BPM, whereby hydroxides and protons from the adjacent flow channels recombine within the membrane to form water molecules. In the discharging period, salt ions also diffuse from solution into the electrodes and ion-exchange layers of the BPM, restoring the ions that were expelled during the charging step (i.e., coions expelled from the electrode and mobile counterions depleted from the BPM). Thus, a dynamic equilibrium state is reached between the BPM, electrode, and solution over repeated charge—discharge cycles.

To clearly demonstrate the outlined principles of the BPMassisted electrosorption process and reduce system complexity, we conducted our initial experiments using single salt solutions (i.e., without the inclusion of boric acid in the feedwater). We performed voltage sweep experiments under reverse bias operation to gain an initial understanding of the transport phenomenon present during charging of the BPM-electrosorption system. A high salt concentration (0.5 M NaCl) was utilized to minimize the contribution of solution resistances to the current and obtain an I-V curve that is primarily representative of only the BPM and electrode charge transfer-related phenomena. By sweeping the voltage from 0.0 to 2.6 V, we obtained an I-V curve with two distinct regimes, which has been shown to be characteristic of BPM water dissociation processes (Figure 2B).<sup>27</sup> Specifically, at relatively low cell potentials (<0.8 V), the current quickly encounters a plateau region where increasing the voltage does not lead to a notable change in the current response. At these low potentials, water dissociation is not yet prevalent, and the majority of the current is carried by the leakage of salt ions across the BPM (i.e., co-ion transport). Beyond 0.8 V, however, the current rapidly increases, indicating the onset of water dissociation at the BPM interfacial junction.

Although the current in this water dissociation region increases quickly with a near quadratic relation, BPM ED (BPED) often shows an even steeper, almost exponential rate of increase in current. The relatively slower rate of increase in current observed in BPM—electrosorption is likely due to the differing electrode charge transfer mechanism. Specifically, in BPED, rapid Faradaic reactions at the electrode surfaces are promoted through the use of strong electrolyte solutions which are applied as electrode rinse solutions, ensuring the electrode reaction is not rate (current) limiting. However, in BPM—electrosorption, the majority of the current is capacitive (for moderate applied voltages), achieved through electrosorption of ions in the electric double layers of the electrodes. Electrosorption, which requires ions to migrate into

the electrode's micropores and be arranged into the electric double layer structure, imposes greater mass transfer resistance as compared to the Faradaic electron transfer in BPED. 32-34 Additionally, in electrosorption, a relatively large potential drop across the EDL structure (i.e., the Stern potential and the Donnan potential) detracts from the effective potential for ion transport. 33,35,36 In effect, electrosorption processes typically provide more modest current values, particularly when compared to multi-cell pair electrodialysis stacks in which the electrode potential (associated with the Faradaic charge transfer reactions) is negligible with respect to the overall stack potential.<sup>21</sup> Nonetheless, the BPM-electrosorption process demonstrates current densities up to 11.2 mA cm<sup>-2</sup>, corresponding to an ideal effluent analyte pH of 12.8 (assuming a 1:1 stoichiometry between electron transfer and BPM water dissociation and that BPM water dissociation is the only pH influencing phenomenon)—well above the  $pK_a$  of boric acid (i.e., 9.1).

We further validate the prevalence of BPM water dissociation by monitoring the change in pH of the analyte and catholyte solutions across three consecutive chargedischarge cycles in batch recirculation operation. Because the water dissociation reaction results in the generation of one hydroxide and one proton, it is expected that the change in pH of the anolyte and catholyte solutions should be equal and opposite. In Figure 2C, we confirm this behavior by evaluating the rate of change in concentration of the hydroxides and protons in the anolyte and catholyte, respectively. During cell charging, the hydroxide and proton concentrations increase rapidly, showing peak rates of generation by 10 min, followed by a gradual decline in the rate of generation for the remainder of the charging period. This variable rate of water dissociation during the charging period provides evidence that the water dissociation reaction is indeed coupled with capacitive electrode processes, as hypothesized. Specifically, the rate of hydroxide and proton generation is the highest following the depletion of priorly stored charge carriers (i.e., mobile counterions) from the ion-exchange layers of the membrane, as this is when water dissociation in the BPM is induced. The rates of hydroxide and proton generation then show a decline over time, as is expected due to the gradual saturation of electrosorption sites. Such behavior is in contrast to steadystate, constant-current processes, such as BPED, where the rate of water dissociation remains constant indefinitely.

Upon short circuiting the cell and switching to discharging mode, the sign of the change in concentration immediately flips, indicating the consumption of hydroxides and protons. The relatively equal consumption rates of hydroxides and protons confirm the occurrence of water reformation at the interfacial junction of the BPM (i.e., forward bias operation). Since the discharging process is solely driven by a concentration gradient in the short-circuit operation mode utilized, the rate of hydroxide and proton consumption asymptotically approaches zero, reflecting the end of water reformation and ion desorption from the electrodes.

The majority of the points in Figure 2C, both in the charging and discharging, agree within the uncertainties of measurement, reinforcing that water dissociation is indeed the dominant mechanism of pH change in the system at moderate applied potentials (1.4 V). However, a notable discrepancy exists at the beginning of the charging cycle (<5 min), during which the rate of proton accumulation in the catholyte is substantially greater than the rate of hydroxide accumulation in

the anolyte. It is important to note that this deviation exists inside the bulk anolyte and catholyte solutions and is therefore not reflective of transient phenomena occurring inside the membrane; thus, the mechanism of water dissociation is not necessarily contradicted. When a BPM is placed under reverse bias operation, the ion exchange layers are initially depleted of mobile counterions, and a new equilibrium is established between the ions inside the membrane—including hydroxides and protons—and the fixed charge groups. 37,38 Hence, during the first few minutes of operation, the generated hydroxides and protons may be exchanged for salt ions and retained in the AEL and CEL, respectively. Ions with a particularly high affinity for a functional group are more highly exchanged in the membrane during this equilibration period, leading to a slower rate of transport through the layer and into solution. It is well known that the mobility of hydroxides is significantly lower than that of protons in ion-exchange membranes,<sup>39</sup> explaining the slower rate of initial hydroxide release from the AEL. Additionally, the ion-exchange layers of BPMs are not necessarily of equal ion exchange capacity and thickness, which would also lead to a difference in each layer's initial rate of ion depletion and duration of equilibration. Hence, we attribute the unequal rate of hydroxide and proton accumulation in solution at the start of the charging step to these transient effects.

We conclude our mechanistic investigation of the BPMelectrosorption process by conducting a full species and charge balance across a charge-discharge cycle in both the anolyte and catholyte under batch recirculation operation. We use (5) mM) sodium bromide as the feed solution for these experiments, as opposed to sodium chloride, to avoid interference from the gradual leakage of the concentrated KCl electrolyte from within the pH probe, which was continuously in solution to monitor the hydroxide and proton concentrations. In Figure 2D, we specifically show the change in the concentration of sodium, bromide, and hydroxide ions in the anolyte, using the concentration at time zero as a reference point. Notably, taking the valence-based sum of the change in concentration of each ion should theoretically equal zero to be in compliance with charge neutrality in solution. Our experimental data agrees well with this condition, with the largest discrepancy from charge neutrality being ~0.1 mmol L-1, which may be attributed to the measurement capabilities of the ion chromatography columns and pH probe.

Upon cell charging, the concentrations of sodium and bromide increase, with the change in the sodium ion concentration being slightly less than that of bromide, and the difference being made up by a small increase in hydroxide concentrations (5 min). Although the concentration change of hydroxide is relatively small compared to that of sodium and bromide for this time point, it should be noted that the pH of the anolyte had nonetheless already increased substantially from 7.3 to 9.4. The behavior of this first time point is in agreement with our proposed mechanism—that at the beginning of the charging step, the dominant mechanisms are co-ion (i.e., Na<sup>+</sup>) expulsion from the electrode and mobile counterion (i.e., Br<sup>-</sup>) release from the AEL of the BPM. Over the remainder of the charging period, in contrast, the sodium ion concentration in solution remains relatively stable, indicating insignificant rates of co-ion expulsion from the electrode. Concurrently, the amount of hydroxide in solution rapidly increases, while bromide is removed from the solution in approximately the same quantity due to electrosorption.

Hence, it can be concluded that BPM-induced water dissociation is indeed highly coupled with electrosorption for the majority of the charging duration. Specifically, the anodic current efficiency  $(\eta_{\rm an})$  for electrosorption versus co-ion expulsion can be approximated as 81% using the following relation, which compares the change in bromide concentration  $(\Delta C_{\rm Br})$  to the sum of the change in bromide concentration and the change in sodium concentration  $\Delta C_{\rm Na}$ 

$$\eta_{\rm an} = \frac{-\Delta C_{\rm Br}}{-\Delta C_{\rm Br} + \Delta C_{\rm Na}} \tag{1}$$

For  $\Delta C_{\rm Br}$ , the change in bromide concentration at the end of the charging cycle is utilized. However, for  $\Delta C_{\rm Na}$ , we use the maximum change in sodium concentration throughout the charging session (i.e., 15 min) to account for potential transfer of sodium from the analyte to catholyte over time via co-ion transport across the BPM.

Once the applied potential is removed and the cell enters the discharging period, it can be seen that sodium is rapidly removed from solution, likely back into the pores of the electrode. Meanwhile, the hydroxide concentration declines as it is consumed for water reformation in the BPM, and the bromide concentration increases as desorption from the electrode proceeds. As the bromide and hydroxide gradually return to their original concentrations (i.e., from before beginning the charging step), the rates of hydroxide consumption and bromide desorption begin to decrease, in accordance with the diminishing concentration gradients in the system. By the end of the discharging period, the concentrations of all species return to near their original values, indicating nearly complete desorption from the electrode and promising the cyclability of the process.

Electrosorption of Boron by the BPM-Electrosorption Process. After gaining an understanding of the fundamental mechanisms involved in charging and discharging the BPM-electrosorption system, the boron removal capability and mechanism were assessed through a series of singlepass experiments using a mixed salt feedwater consisting of sodium chloride and boric acid (5 mM NaCl, 1 mM B(OH)<sub>3</sub>). A single-pass configuration was used for the remainder of the experiments to best represent the practical operation of the process. We note that we used a slightly higher boron concentration for the feedwater, compared to that typically encountered in the permeate of first pass seawater RO (<0.5 mM), to most clearly gauge the boron removal capacity of the system, while still remaining within an environmentally relevant range. As discussed in the prior investigation of process mechanisms, ions may be sorbed by either the electrode during cell charging or by the BPM during discharging. Therefore, in addition to determining if the process is capable of removing boron, it is also critical to determine the fate of the boron in the system.

In an effort to see the largest change in boron concentration, we began our boron removal performance testing by applying 2.6 V, the maximum potential tested in our linear sweep voltammetry experiments (Figure 2B). Figure 3 (blue data points) presents the change in boron concentration over three consecutive charge—discharge cycles, with discharging completed at 0 V. At the beginning of the charging period, the boron concentration slightly increases, as borate stored in the AEL is released into solution (while the BPM is depleted of mobile counterions). By 5 min into the charging period,

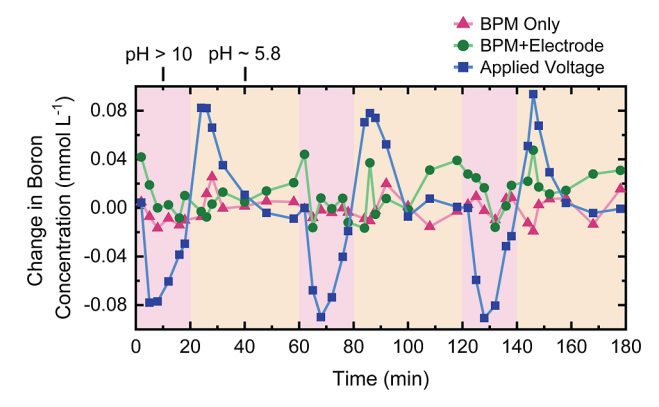


Figure 3. Confirmation of boron removal with the BPM-electrosorption system and elucidation of the boron removal mechanism. Feedwater consisting of 5 mM NaCl and 1 mM B(OH)<sub>3</sub> was fed to the system at a flowrate of 1.0 mL min<sup>-1</sup> in a single-pass configuration. The change in the boron concentration for three consecutive cycles is shown for the case where an external voltage is applied (2.6 V, blue points) and where no voltage is applied but the feedwater pH is manually adjusted through chemical addition. Two scenarios without an applied voltage are investigated: when the BPM-electrosorption cell consists of all the required components (i.e., BPM + electrodes, green points) and when the cell consists of only the BPM (i.e., the electrodes are removed, pink points). Durations where the cell is operating under high pH conditions are shown in the pink background, whereas durations during which the feedwater pH is not adjusted are shown in the orange background.

however, we observe a significant decrease in the boron concentration of the effluent, indicating effective removal by the BPM—electrosorption system. Over the remainder of the charging time, boron continues to be removed, although to a diminishing extent as the anode begins to saturate with ions. When the cell is short-circuited, the boron concentration immediately spikes well above the feed concentration, representing desorption of boron from the electrodes. As the concentration gradient of boron between the pores of the electrode and the feed solution lessens over time, the desorption of boron eventually ceases.

As seen in Figure 3, the sorption and desorption of boron were highly reproducible across the three consecutive cycles. Integration of the charging peaks with respect to time gives an average specific removal capacity of 4.99  $\pm$  0.19  $\mu \rm mol~g^{-}C^{-1}$ , significantly higher than prior studies using flow-through electrosorption. Similarly, integrating the discharging peaks reveals high regenerability of the anode, with an average 87  $\pm$  12% desorption rate of boron. We note that when using only concentration gradients as the driving force (i.e., 0 V) for desorption, discharging durations slightly longer than the charging period may be required, as suggested by the asymmetric cycle timing (i.e., 20 min charge and 40 min discharge) used in our single-pass experiments. Nonetheless, the kinetics of desorption may be accelerated by applying a reverse potential or current.

To ensure the observed removal of boron is achieved through electrosorption, as opposed to physi- or chemisorption in the electrodes or BPM, we conducted a series of rigorous control experiments where no electric potential was applied. Specifically, we performed controls in which the BPM– electrosorption system was assembled with all its components ("BPM + electrode") and where the carbon electrodes were removed from the system ("BPM only") to assess the relative

impact of both the electrodes and the membrane on boron removal. To encompass the effects of the pH swings encountered in a typical charge—discharge cycle (i.e., applied voltage for charging and 0 V discharging), the control experiments consisted of periodically switching the feedwater between a pH 10 solution and an unadjusted pH solution (pH  $\sim 5.8$ ), corresponding to the charging and discharging periods, respectively. At a pH of 10, effectively all the boron in solution is ionized, whereas at pH 5.8, boron is present predominantly as the uncharged boric acid. Thus, any adsorption and desorption related to the swinging of the pH and boron ionization degree should theoretically be captured by these experiments.

With only the BPM (pink data points in Figure 3), the boron concentration does not show any notable change or trend throughout the durations of high pH and neutral pH. The deviation which is observed may largely be attributed to the measurement error of the ICP-MS. The BPM's lack of boron uptake was further evidenced by its low preference for borate over chloride ions, as determined by an ion-exchange test (Figure S5). Specifically, the AEL of the BPM was converted to hydroxide form (i.e., all the counterions in the ion-exchange layer were exchanged for hydroxide ions), and a solution of 5 mM NaCl and 1 mM B(OH)3 at pH 10 was recirculated along the AEL to determine the relative uptake of borate and chloride ions over time. The borate removed from solution, and hence exchanged for hydroxide in the membrane, was found to be negligible compared to the uptake of chloride ions, thus demonstrating a relatively low affinity of borate ions toward the chemical composition of the membrane.

The control experiments which included both the carbon electrodes and BPM showed a larger deviation in boron concentration, as can be seen by the green data points in Figure 3. Nonetheless, a clear trend is still not discernible. Furthermore, it should be noted that most of the points, both in the high and neutral pH conditions, are positive in magnitude, indicating some release of boron but no notable removal. We further assessed the significance of boron adsorption on the carbon electrodes through attenuated total reflectance Fourier transform infrared spectroscopy (ATR-FTIR) characterization of the anode and cathode before and after use in a single-pass boron electrosorption experiment. The spectra of the electrode (Figure S6) show little difference after being exposed to the boron-containing feed solution during the experiment. Although a peak near 2950 cm<sup>-1</sup> is introduced in both the anode and cathode after the experiment, this wavenumber does not correspond to boron, indicating inconsequential amounts of adsorption and further supporting the results of our control experiment. Thus, it can be concluded that electrosorption is indeed the dominant mechanism for boron removal under an applied voltage, with adsorption in the BPM and electrodes playing an insignificant role toward overall removal.

**Determination of Optimal Voltage.** The effect of applied voltage on the boron removal performance of BPM–electrosorption was investigated. Specifically, cell potentials ranging from 1.0 to 2.6 V were tested, in accordance with the water dissociation window determined in Figure 2B. Intuitively, increasing the applied potential should increase the capacity of the electric double layers, resulting in a larger degree of electrosorption of all ions, including borate. However, as shown in the bottom panel of Figure 4A, the specific capacity of the anode for boron  $(\Gamma_{\rm R})$  does not follow

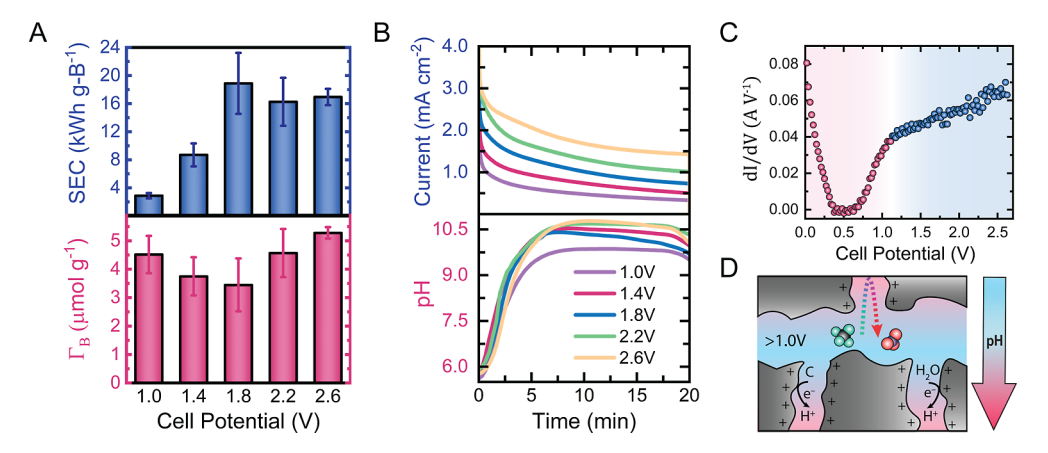


Figure 4. Dependence of process performance on the applied cell voltage. Feedwater consisting of 5 mM NaCl and 1 mM B(OH)<sub>3</sub> was fed to the system in a single-pass configuration at a flowrate of 1.0 mL min<sup>-1</sup> throughout. (A) Specific boron sorption capacity ( $\Gamma_B$ ) and corresponding specific energy consumption (SEC) for each applied voltage. (B) Measured response of the current and the pH over the charging duration for each of the applied voltages. (C) Change in the current with respect to voltage over a range of cell potentials. Two regimes are shown, indicating the approximate voltage at which proton-generating anodic reactions are expected to become prevalent. Current vs voltage data was obtained from linearly sweeping the voltage at a 5 mV s<sup>-1</sup> scan rate with a feedwater concentration of 500 mM NaCl. (D) Schematic illustration showing the theorized mechanism for hindered borate electrosorption at high cell potentials. Although the pH in bulk solution is sufficiently high for the existence of borate ions, the pH in the micropores of the electrode may decrease at high applied voltages due to the occurrence of protongenerating Faradaic reactions at the anode, thus back-converting borate (blue tetrahedral molecule) to boric acid (red trigonal planar molecule) and preventing effective boron electrosorption.

the expected monotonic trend. Rather, we observe a parabolic relation whereby increasing the cell potential above 1.0 V initially results in a decline in boron removal performance, followed by gradual restoration in the sorption capacity at higher voltages. Specifically, increasing the charging voltage from 1.0 to 1.8 V results in a 23.7% loss in sorption capacity, while further increasing the potential to 2.6 V leads to a 17.1% greater boron removal compared to 1.0 V operation. Accordingly, a tradeoff between boron removal performance and applied voltage is apparent.

The parabolic relation observed between boron removal and applied potential may be rationalized through assessment of the current and pH data at each applied voltage (Figure 4B). As the potential is stepped up from 1.0 to 2.6 V, the current response shows a consistent, proportional increase. Assuming this rise in current translates to a faster rate of water dissociation in the BPM—as suggested by our investigation of process mechanisms in previous sections—the hydroxide concentration in the analyte is also expected to increase. Stepping the voltage up from 1.0 to 1.4 V confirms this expected behavior, increasing the maximum analyte pH from 9.86 to 10.53. Notably, the elevated pH at 1.4 V corresponds to a hydroxide concentration (~0.32 mM) within the same order of magnitude as the concentration of ionized boron ( $\sim$ 1.0 mM). Thus, increasing the potential above 1.0 V greatly exacerbates competition between borate and hydroxide ions for electrosorption sites on the anode, which may explain the drop in boron sorption capacity at 1.4 V. With hydroxide ions having an inherent advantage over borate for electrosorption due to their substantially greater mobility in solution, the pH of the anolyte should ideally be maintained between 9 and 10 to ensure maximal ionization of boron, while minimizing competition with hydroxide ions.

Although a drastic increase in the pH is observed upon increasing the applied voltage from 1.0 to 1.4 V, further increasing the voltage from 1.4 to 1.8 V surprisingly leads to an inverse trend, whereby the pH of the analyte slightly decreases. Furthermore, the pH profile for 1.8 V shows a prominent

downward slope, decreasing from a pH of 10.41 to 9.68 over the last 10 min of charging. The pH profiles of 1.0 and 1.4 V are, in contrast, much more stable over the charging duration. These anomalous features in the pH profile of 1.8 V indicate the occurrence of additional pH-influencing mechanisms apart from BPM water dissociation and electrosorption.

It is well known that when the cell potential is increased above 1.4 V in electrosorption processes, Faradaic charge transfer becomes increasingly prevalent and detrimental to charge efficiency. Hence, the drop in boron sorption capacity and the unexpected behavior in pH may be attributed to the onset and occurrence of these Faradaic reactions. In particular, proton-generating reactions at the anode, such as the oxidation of the carbon electrode (eq 2) and water splitting (eq 3), 40,41 are of particular interest for boron removal, as they are not only counterproductive toward charge efficiency (like in classical electrosorption processes) but also result in neutralization of the hydroxides produced by BPM water dissociation

$$C + 2H_2O \rightarrow CO_2 + 4H^+ + 4e^- \qquad E^0 = 0.21 \text{ V/SHE}$$
 (2)

$$2H_2O \rightarrow O_2 + 4H^+ + 4e^- \qquad E^0 = 1.23 \text{ V/SHE}$$
 (3)

In Figure 4C, we approximate the voltage at which significant Faradaic charge transfer occurs in the BPM–electrosorption system by taking the derivative of the current with respect to voltage from a voltammetry sweep. An inflection in the slope, accompanied by progressively greater scattering of data points, is observed around 1.1 V, signifying the presence of considerable Faradaic charge transfer. Hence, at cell potentials above  $\sim 1.0$  V, proton generation at the anode is expected to be of concern—either from carbon oxidation or water splitting.

With Faradaic reactions, and thus generation of protons, primarily occurring in the micropores of the electrode, a substantial pH gradient is likely to develop between the macropores (i.e., bulk solution pH) and the micropores of the anode, whereby the pH in the electrode's micropores is lower

than in bulk solution, as depicted in Figure 4D. 41,42 Such pH gradients have been observed in studies of conventional electrosorption and are likely to be even more severe in the case of BPM—electrosorption due to the anode continuously being exposed to high pH conditions, under which the carbon oxidation and oxygen evolution reactions are more thermodynamically favorable (i.e., reduction potentials become more negative). 41 Depending on the pervasiveness of Faradaic proton generation, borate ions which are ionized in bulk solution may undergo back-conversion to boric acid as they enter the more acidic electrode micropores (Figure 4D), effectively hindering boron electrosorption and resulting in lower sorption capacity despite an increase in applied voltage.

According to the logic presented above, increasing the cell potential from 1.8 to 2.2 and 2.6 V should further induce parasitic anode reactions, leading to greater deterioration in boron sorption capacity. However, in these cases, we observe a gradual enhancement in boron electrosorption performance. Furthermore, with each step up in potential, the pH continues to rise to higher peak values and shows good stability over the charging duration compared to operation at 1.8 V. Thus, it may be inferred that for these voltage steps, the rate of increase in anodic Faradaic reactions (proton generation) is outweighed by a more significant rate of increase in BPM water dissociation (hydroxide generation). Nonetheless, to maximize the longevity of electrode performance, Faradaic reactions, particularly carbon oxidation, should be mitigated through the application of lower applied potentials.

Because of the intricate relation between boron sorption capacity and applied voltage, the determination of an optimal operating voltage is nontrivial. Thus, we utilize the SEC—the energy consumption normalized by the amount of boron removed—for further process evaluation and optimization. The energy consumption, given by the numerator of eq 4, is calculated by taking the product of the applied voltage (V) and the integral of the current (I) over the charging duration  $(t_c)$  with respect to time (i.e., total charge transferred). The SEC is then determined by normalizing the energy consumption by the total amount of boron removed, given by integrating the difference between the feed boron concentration  $(C_{\rm B,0})$  and the effluent boron concentration  $(C_{\rm B})$  over the charging step and multiplying by the volumetric feed flow rate (Q).

SEC = 
$$\frac{V \int_0^{t_c} I \, dt}{Q \int_0^{t_c} (C_{B,0} - C_B) \, dt}$$
 (4)

The energy consumption is normalized by the mass of boron removed, rather than the volume of water treated, due to the relatively small extents of boron removal achieved by the laboratory-scale flow cell and the transient effluent conditions inherent of constant voltage operation. The accurate determination of a volume-normalized energy consumption will require more realistic operation in constant current mode and the use of a significantly larger active area to augment the cell's boron removal capability to reach the boron removal extents required for achieving regulatory guidelines. Nonetheless, boron mass-normalized SEC values still serve as an appropriate metric for the initial evaluation of process performance.

The SEC of each applied voltage, shown in the top panel of Figure 4A, reveals that charging at 1.0 V provides the most efficient boron removal, with an SEC of 2.88 kWh per gram of

boron electrosorbed (g-B<sup>-1</sup>). In contrast, operation at 1.8 V requires more than sixfold the energy consumption, due to the increased current and voltage but a lower extent of boron removal. Although the sorption capacity of boron at 2.2 and 2.6 V is greater than at 1.0 V, the advantage in boron removal is not proportional to the substantial increase in potential and current, thus resulting in relatively high-energy consumptions of 16.3 and 16.9 kWh g-B<sup>-1</sup>, respectively. Hence, 1.0 V is determined to be the optimal voltage for boron electrosorption, with the remainder of experiments being carried out at this cell potential.

Comparison of Electrosorption Configurations for Boron Removal. To assess whether the incorporation of a BPM provides a significant advantage toward electrosorption of boron, we compared the boron removal performance of BPM-electrosorption to alternative electrosorption configurations. Specifically, the performance of traditional flow-by electrosorption and flow-through electrosorption—a configuration which has recently been demonstrated for boron removal<sup>22</sup>—were evaluated alongside BPM-electrosorption. A fair comparison was ensured between each configuration by keeping all operating parameters (i.e., feedwater composition, applied voltage, charging and discharging duration, and flowrate) equal. The design and materials used in the construction of each cell were also kept as similar as possible, with details provided in the Supporting Information, to further guarantee a meaningful assessment. Each of the experiments conducted for the comparison of electrosorption configurations was completed in a single-pass configuration using the same experimental protocol.

To gain insights into the process dynamics of each configuration, the boron concentration was monitored over time for the first charge-discharge cycle of each triplicate set. Accordingly, in Figure 5A, we overlay the change in boron concentration over time for each configuration. It is immediately apparent that in the flow-by configuration, the boron concentration does not effectively change across both the charge and discharge durations, showing only negligible fluctuations that may be attributed to error in ICP-MS measurements. This result is sensible since in conventional flow-by operation, a high solution pH is not attained, and thus boric acid is not ionized or electrosorbed at the anode. In fact, monitoring the effluent from the flow-by cell showed a drop in pH during the charging period, further deterring effective boron electrosorption. With flow-by electrosorption being deemed ineffective for boron removal (without the addition of chemicals to increase the pH), we did not perform any additional analysis on its performance.

For flow-through electrode experiments, the anode was placed upstream of the cathode, as this orientation has recently been demonstrated to promote the removal of boron. Specifically, it has been theorized that in such a configuration, there is a spike in pH at the anode—separator interface, which facilitates boron ionization and electrosorption. This locally increased pH has been attributed to several phenomena, including differences in the mobility and electrosorption rates of protons and hydroxides, acid—base equilibria with surface functional groups, and water dissociation reactions. Although successful boron removal was demonstrated both theoretically and experimentally in this study, the boron sorption capacity remained marginal across various operating conditions, with optimized performance showing <1  $\mu$ mol g<sup>-1</sup> removal and

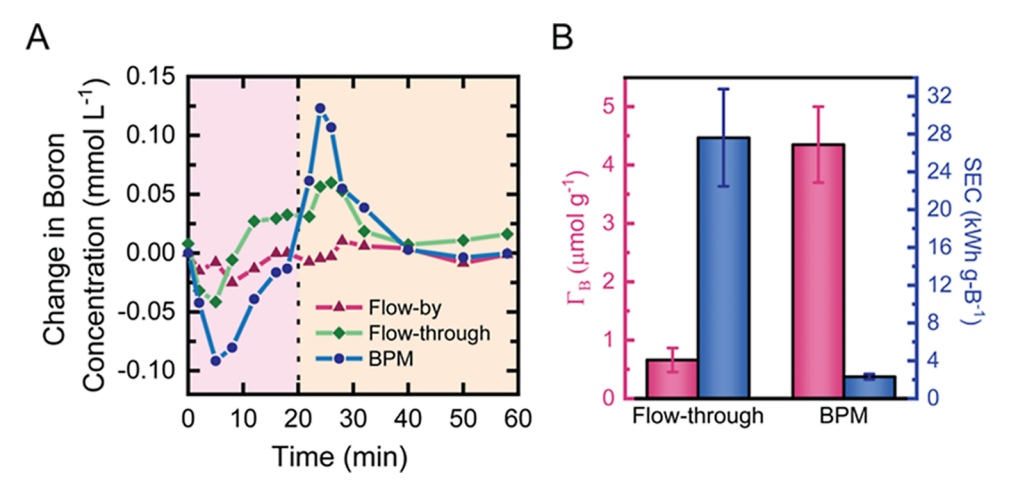


Figure 5. Comparison of the boron removal performance between the BPM–electrosorption system and alternate electrosorption configurations. Feedwater consisting of 5 mM NaCl and 1 mM B(OH)<sub>3</sub> was fed to each of the systems in a single-pass configuration at a flowrate of 1.0 mL min<sup>-1</sup>. (A) Boron concentration over a charge–discharge cycle for flow-by electrosorption (pink), flow-through electrosorption (green), and BPM–electrosorption (blue). The charging duration is shown in the pink background, whereas discharging is shown in the orange background. (B) Comparison of the boron sorption capacity and SEC of flow-through electrosorption and BPM–electrosorption. Pink bars show the specific boron sorption capacity, while blue bars show the SEC.

many other conditions resulting in non-sensible negative removal values.

In our flow-through electrode experiments, when an electric potential was applied, the boron concentration decreased rapidly over the first 5 min (Figure 5A), representing electrosorption. However, by 12 min of charging, the concentration of boron in the effluent was higher than in the feed, indicating premature desorption of boron. Such desorption may be due to an unstable pH in the anode, whereby a drop of the anodic pH causes back-conversion of borate to boric acid and subsequent reversal of electrosorption. When the cell is short circuited (i.e., discharged), a moderate spike in the boron concentration is observed, as the remaining borate on the electrode is desorbed. Nonetheless, with the relatively small changes in boron concentration and the presence of unexpected desorption in the charging step, it remains unclear whether boron is effectively electrosorbed in the anode or if the observed changes in boron concentration are largely an effect of a dynamic adsorption equilibrium on the carbon electrodes due to the transient pH conditions—and hence degree of boron ionization—in the flow-through system.

Overall, our flow-through electrosorption results indicate small extents of boron removal, with an average specific capacity of only 0.66 µmol per gram of carbon electrode, in close agreement with the boron sorption capacity values recently published.<sup>22</sup> In contrast, the BPM-electrosorption system demonstrated a remarkably higher boron sorption capacity of 4.35 µmol per gram of carbon—nearly a sevenfold improvement in performance (Figure 5B). The drastic difference in boron removal performance may largely be due to more effective and reliable generation of hydroxide in BPM-electrosorption as compared to flow-through electrosorption. Specifically, in BPM-electrosorption, the pH of the entire anolyte compartment (i.e., both the bulk solution and solution inside the anode) is effectively increased. In flowthrough electrosorption, however, only the portion of the anode at the electrode-separator interface is at high pH conditions, while the remainder of the anode remains acidic.<sup>2</sup> Thus, the effective electrode area for borate electrosorption in a flow-through configuration is severely limited.

To further assess the performance of BPM-electrosorption with respect to flow-through electrosorption, we also determined the SEC of each configuration, as shown by the blue bars in Figure 5B. Provided the same voltage, flowthrough electrosorption shows a significantly larger current response than BPM-electrosorption (Figure S7)—despite its much lower removal of boron. The higher current observed in flow-through electrosorption may be attributed to its less regulated ion transport mechanisms as compared to those of BPM-electrosorption. Specifically, in BPM-electrosorption, electrode processes (i.e., co-ion expulsion, electrosorption, and Faradaic reactions) are directly coupled with water dissociation in the BPM, thus constraining the rate of ion transport and current. However, in flow-through electrosorption, such a pairing is not imposed, resulting in comparatively lower ion transport limitations which facilitates greater currents. Accordingly, flow-through electrosorption transfers over twice the amount of charge as BPM-electrosorption over the same charging duration, thus corresponding to over twice the energy consumption. Normalizing the energy consumption to the amount of boron removed further differentiates the performance of each configuration, with flow-through electrosorption consuming over an order of magnitude more energy per gram of boron removed.

Another electrosorption configuration that has recently demonstrated boron removal capability resembles membranecapacitive deionization (MCDI).<sup>23</sup> However, unlike conventional MCDI, only an anion-exchange membrane is placed in front of the anode, while the cathode remains bare. Thus, when sufficiently high potentials are applied (i.e., >2.0 V used in the study), oxygen reduction and water splitting are induced at the cathode, in turn producing hydroxide ions which migrate to the flow channel. The pH of the feed stream is thereby increased, effectively ionizing boron, which can then migrate to the anode. Although not thoroughly discussed in the study, water and carbon oxidation reactions will simultaneously occur at the anode, generating protons, which are largely blocked from entering the flow channel by the anion-exchange membrane. Thus, a gradually more acidic pH in the anode is expected to develop over the charging duration, in effect

contradicting the proposed mechanism of boron electrosorption. Specifically, although borate ions may exist in the high pH conditions of the flow channel—hence facilitating the electromigration of boron into the anode—the borate ions are likely to be back-converted into boric acid once inside the pores of the anode. The uncharged boric acid is thereby effectively trapped by the anion-exchange membrane and is unable to re-enter the flow channel. The mechanism of boron removal in this process may therefore be considered to be more electrodialytic than capacitive in nature. Additionally, the process utilizes a reverse current in order to achieve boron desorption since reversing the electrode polarity creates the local basic environment (at the cathode) required to re-ionize the trapped boric acid and facilitate its transport back through the anion-exchange membrane into solution. Hence, in this process, energy input is required in both the charging and discharging steps, unlike in BPM-electrosorption. Furthermore, the process' reliance on Faradaic reactions at the cathode for pH adjustment necessitates relatively high potentials (i.e., generally above the water splitting potential), which has been shown to be detrimental for the long-term stability of carbon electrodes in electrosorption processes. <sup>18</sup> In contrast, BPM-electrosorption does not depend on cathodic reduction reactions, instead using a water dissociation mechanism to generate hydroxide ions, enabling efficient operation at lower potentials (with the optimal voltage being determined as 1.0 V in the previous section). Thus, BPMelectrosorption is expected to provide greater promise for stable long-term performance.

#### ■ ENVIRONMENTAL IMPLICATIONS

Boron removal from aqueous solutions has long persisted as a technical challenge, still requiring the use of chemical- and energy-intensive processes to meet water quality standards. In this study, we introduced a novel electrochemical technology which combines the unique features of BPMs and capacitive electrodes to effectively remove boron and complete all required pH adjustments in a chemical-free manner. The BPM-electrosorption process shows promising boron sorption capacity compared to alternative electrosorption methods and is capable of operating at relatively low SEC values (~2.5 kWh g-B<sup>-1</sup>). However, larger-scale testing, in which operation is more rigorously optimized, energy recovery during discharging is considered, and boron is more extensively removed, will be required for direct comparison with the energy consumption of the current state-of-the-art method, multi-pass RO.

The feedwater conditions utilized throughout the majority of this study (i.e., 5 mM NaCl and 1 mM B(OH)<sub>3</sub>) demonstrate that the BPM-electrosorption technology is well suited for treatment of first-pass seawater RO permeate. Additionally, preliminary experiments using various boron and salt concentrations suggest that the process is flexible in terms of applicability (Figure S8). Specifically, the BPM-electrosorption process showed effective boron removal for salt concentrations as low as 1 mM sodium chloride and boron concentrations ranging from 0.5 to 2 mM. Hence, BPMelectrosorption may also be extended to applications which consist of low background electrolyte concentrations, such as the production of ultrapure water. Enhancing the selectivity of boron electrosorption over competing anions found in natural waters (e.g., chloride) may also enable direct application of the technology toward waters with higher ionic strength, such as

contaminated groundwaters and lithium-rich brines. However, because the energy consumption and boron removal performance are expected to be highly dependent on the feed solution conductivity, ionic composition, and buffering capacity, further investigation is necessary to effectively determine the most efficient feedwater for the technology.

A key advantage the BPM-electrosorption technology provides with respect to alternate boron removal methods is the ability to achieve in situ elevation of pH followed by subsequent neutralization of the product water pH in a single process. Specifically, in BPM-electrosorption, water dissociation by the BPM generates hydroxide ions in the anolyte channel while simultaneously producing protons in the catholyte. Although the two chambers are separated from one another by the water impermeable BPM, the anolyte and catholyte may be hydraulically connected by feeding the cathode chamber with the high pH, boron-depleted anolyte effluent. Thus, the protons generated by BPM water dissociation may be utilized to restore the pH of the final product water to circumneutral. Such capability is not offered in other electrosorption techniques, which utilize only one flow channel and are thereby restricted to a high pH product water, which must later be neutralized through additional processing steps. BPED configurations are similarly limited to high pH product waters since in ED, the boron is transferred from the feed chamber to the adjacent receiving chamber (where protons are generated by the BPM), rather than being stored in electrodes (i.e., BPM-electrosorption).<sup>43</sup> Hence, the high pH product water may not be passed through the acidic chamber without re-contaminating the water with boron. The BPM-electrosorption process thus offers the unique ability to "electrify" all necessary pH adjustments, overcoming a major environmental limitation of boron removal with both multipass RO and ion-exchange resins.

#### ASSOCIATED CONTENT

#### Supporting Information

The Supporting Information is available free of charge at https://pubs.acs.org/doi/10.1021/acs.est.3c00058.

Membrane and electrode pretreatment; flow-through and flow-by cell designs; pore size distribution of activated carbon cloth electrode material; design and photograph of flow-through electrosorption cell; photograph of single-pass BPM-electrosorption setup; photograph of batch mode BPM-electrosorption setup; ion-exchange capacity test of BPM; ATR-FTIR spectra of carbon cloth before and after experiments; current response of flow-through and BPM-electrosorption experiments; and effect of feedwater composition on boron sorption capacity (PDF)

#### AUTHOR INFORMATION

#### **Corresponding Author**

Menachem Elimelech – Department of Chemical and Environmental Engineering, Yale University, New Haven, Connecticut 06520-8286, United States; ⊚ orcid.org/0000-0003-4186-1563; Phone: +1 (203) 432-2789; Email: menachem.elimelech@yale.edu

#### **Authors**

Sohum K. Patel – Department of Chemical and Environmental Engineering, Yale University, New Haven,

- Connecticut 06520-8286, United States; o orcid.org/0000-0001-5228-9449
- Weiyi Pan Department of Chemical and Environmental Engineering, Yale University, New Haven, Connecticut 06520-8286, United States; orcid.org/0000-0001-6587-1040
- Yong-Uk Shin Department of Chemical and Environmental Engineering, Yale University, New Haven, Connecticut 06520-8286, United States
- Jovan Kamcev Department of Chemical Engineering, University of Michigan, Ann Arbor, Michigan 48109, United States; Occid.org/0000-0003-0379-5171

Complete contact information is available at: https://pubs.acs.org/10.1021/acs.est.3c00058

#### Notes

The authors declare no competing financial interest.

#### ACKNOWLEDGMENTS

This material is based upon work supported by the National Alliance for Water Innovation (NAWI), funded by the U.S. Department of Energy, Energy Efficiency, and Renewable Energy Office, Advanced Manufacturing Office under Funding Opportunity Announcement DE-FOA-0001905. The work is also supported by the U.S. National Science Foundation (NSF) and U.S.-Israel Binational Science Foundation (BSF) under award no. CBET-2001219. We also acknowledge the American Membrane Technology Association (AMTA) and Bureau of Reclamation fellowship for Membrane Technology awarded to S.K.P.

## ■ REFERENCES

- (1) USEPA. Drinking Water Health Advisory for Boron and Compounds; U.S. Environmental Protection Agency (EPA), 2008.
- (2) Sedlak, D.; Mauter, M.; Macknick, J.; Stokes-Draut, J.; Fiske, P.; Agarwal, D.; Borch, T.; Breckenridge, R.; Cath, T.; Chellam, S. National Alliance for Water Innovation (NAWI) Master Technology Roadmap; National Renewable Energy Laboratory (NREL): Golden, CO, United States, 2021.
- (3) Tagliabue, M.; Reverberi, A. P.; Bagatin, R. Boron removal from water: needs, challenges and perspectives. *J. Cleaner Prod.* **2014**, *77*, 56–64.
- (4) Yáñez-Fernández, A.; Inestrosa-Izurieta, M. J.; Urzúa, J. I. Concurrent magnesium and boron extraction from natural lithium brine and its optimization by response surface methodology. *Desalination* **2021**, *517*, 115269.
- (5) Lu, P. C.; Song, X. F.; Chen, H.; Sun, Y. Z.; Yu, J. G. The Effect of Boron Forms on the Crystallization Process of Lithium Carbonate. *Cryst. Res. Technol.* **2020**, *55*, 1900169.
- (6) Elimelech, M.; Phillip, W. A. The Future of Seawater Desalination: Energy, Technology, and the Environment. *Science* **2011**, 333, 712–717.
- (7) Greenlee, L. F.; Lawler, D. F.; Freeman, B. D.; Marrot, B.; Moulin, P. Reverse osmosis desalination: Water sources, technology, and today's challenges. *Water Res.* **2009**, *43*, 2317–2348.
- (8) Hilal, N.; Kim, G. J.; Somerfield, C. Boron removal from saline water: A comprehensive review. *Desalination* **2011**, 273, 23–35.
- (9) Xu, Y.; Jiang, J. Q. Technologies for boron removal. *Ind. Eng. Chem. Res.* **2008**, 47, 16–24.
- (10) Bick, A.; Oron, G. Post-treatment design of seawater reverse osmosis plants: boron removal technology selection for potable water production and environmental control. *Desalination* **2005**, *178*, 233–246.

- (11) Lokiec, F.; Kronenberg, G. South Israel 100 million m(3)/y seawater desalination facility: build, operate and transfer (BOT) project. *Desalination* **2003**, *156*, 29–37.
- (12) Rybar, S.; Boda, R.; Bartels, C. Split partial second pass design for SWRO plants. *Desalin. Water Treat.* **2010**, *13*, 186–194.
- (13) Li, X.; Liu, R.; Wu, S.; Liu, J.; Cai, S. S.; Chen, D. S. Efficient removal of boron acid by N-methyl-D-glucamine functionalized silicapolyallylamine composites and its adsorption mechanism. *J. Colloid Interface Sci.* **2011**, *361*, 232–237.
- (14) Wei, Y. T.; Zheng, Y. M.; Chen, J. P. Design and fabrication of an innovative and environmental friendly adsorbent for boron removal. *Water Res.* **2011**, *45*, 2297–2305.
- (15) Kamcev, J.; Taylor, M. K.; Shin, D. M.; Jarenwattananon, N. N.; Colwell, K. A.; Long, J. R. Functionalized Porous Aromatic Frameworks as High-Performance Adsorbents for the Rapid Removal of Boric Acid from Water. *Adv. Mater.* **2019**, *31*, 1808027.
- (16) Çelik, Z. C.; Can, B. Z.; Kocakerim, M. M. Boron removal from aqueous solutions by activated carbon impregnated with salicylic acid. *J. Hazard. Mater.* **2008**, *152*, 415–422.
- (17) Oren, Y. Capacitive delonization (CDI) for desalination and water treatment—past, present and future (a review). *Desalination* **2008**, 228, 10–29.
- (18) Landon, J.; Gao, X.; Omosebi, A.; Liu, K. L. Progress and outlook for capacitive deionization technology. *Curr. Opin. Chem. Eng.* **2019**, 25, 1–8.
- (19) Suss, M. E.; Porada, S.; Sun, X.; Biesheuvel, P. M.; Yoon, J.; Presser, V. Water desalination via capacitive deionization: what is it and what can we expect from it? *Energy Environ. Sci.* **2015**, *8*, 2296–2319.
- (20) Qin, M. H.; Deshmukh, A.; Epsztein, R.; Patel, S. K.; Owoseni, O. M.; Walker, W. S.; Elimelech, M. Comparison of energy consumption in desalination by capacitive deionization and reverse osmosis. *Desalination* **2019**, *455*, 100–114.
- (21) Patel, S. K.; Qin, M.; Walker, W. S.; Elimelech, M. Energy Efficiency of Electro-Driven Brackish Water Desalination: Electro-dialysis Significantly Outperforms Membrane Capacitive Deionization. *Environ. Sci. Technol.* **2020**, *54*, 3663–3677.
- (22) Shocron, A. N.; Guyes, E. N.; Rijnaarts, H. H. M.; Biesheuvel, P. M.; Suss, M. E.; Dykstra, J. E. Electrochemical removal of amphoteric ions. *Proc. Natl. Acad. Sci. U.S.A.* **2021**, *118*, No. e2108240118.
- (23) Sun, J. Y.; Zhang, C. Y.; Song, Z.; Waite, T. D. Boron Removal from Reverse Osmosis Permeate Using an Electrosorption Process: Feasibility, Kinetics, and Mechanism. *Environ. Sci. Technol.* **2022**, *56*, 10391–10401.
- (24) Lopalco, A.; Lopedota, A. A.; Laquintana, V.; Denora, N.; Stella, V. J. Boric Acid, a Lewis Acid With Unique and Unusual Properties: Formulation Implications. *J. Pharmaceut. Sci.* **2020**, *109*, 2375–2386.
- (25) Trivedi, G. S.; Shah, B. G.; Adhikary, S. K.; Indusekhar, V. K.; Rangarajan, R. Studies on bipolar membranes. *React. Funct. Polym.* **1996**, 28, 243–251.
- (26) Strathmann, H.; Krol, J. J.; Rapp, H. J.; Eigenberger, G. Limiting current density and water dissociation in bipolar membranes. *J. Membr. Sci.* **1997**, 125, 123–142.
- (27) Ramírez, P.; Rapp, H. J.; Reichle, S.; Strathmann, H.; Mafé, S. Current-voltage curves of bipolar membranes. *J. Appl. Phys.* **1992**, *72*, 259–264.
- (28) Pärnamäe, R.; Mareev, S.; Nikonenko, V.; Melnikov, S.; Sheldeshov, N.; Zabolotskii, V.; Hamelers, H. V. M.; Tedesco, M. Bipolar membranes: A review on principles, latest developments, and applications. *J. Membr. Sci.* **2021**, *617*, 118538.
- (29) Blommaert, M. A.; Aili, D.; Tufa, R. A.; Li, Q. F.; Smith, W. A.; Vermaas, D. A. Insights and Challenges for Applying Bipolar Membranes in Advanced Electrochemical Energy Systems. *ACS Energy Lett.* **2021**, *6*, 2539–2548.
- (30) Ran, J.; Wu, L.; He, Y. B.; Yang, Z. J.; Wang, Y. M.; Jiang, C. X.; Ge, L.; Bakangura, E.; Xu, T. W. Ion exchange membranes: New developments and applications. *J. Membr. Sci.* **2017**, *522*, 267–291.

- (31) Vermaas, D. A.; Smith, W. A. Synergistic Electrochemical CO2 Reduction and Water Oxidation with a Bipolar Membrane. ACS Energy Lett. 2016, 1, 1143-1148.
- (32) Salamat, Y.; Hidrovo, C. H. Significance of the micropores electro-sorption resistance in capacitive deionization systems. Water Res. 2020, 169, 115286.
- (33) Wang, L.; Dykstra, J. E.; Lin, S. H. Energy Efficiency of Capacitive Deionization. Environ. Sci. Technol. 2019, 53, 3366-3378. (34) Qu, Y. T.; Baumann, T. F.; Santiago, J. G.; Stadermann, M. Characterization of Resistances of a Capacitive Deionization System. Environ. Sci. Technol. 2015, 49, 9699-9706.
- (35) Hemmatifar, A.; Ramachandran, A.; Liu, K.; Oyarzun, D. I.; Bazant, M. Z.; Santiago, J. G. Thermodynamics of Ion Separation by Electrosorption. Environ. Sci. Technol. 2018, 52, 10196-10204.
- (36) Patel, S. K.; Ritt, C. L.; Deshmukh, A.; Wang, Z. X.; Qin, M. H.; Epsztein, R.; Elimelech, M. The relative insignificance of advanced materials in enhancing the energy efficiency of desalination technologies. Energy Environ. Sci. 2020, 13, 1694-1710.
- (37) Bui, J. C.; Digdaya, I.; Xiang, C. X.; Bell, A. T.; Weber, A. Z. Understanding Multi-Ion Transport Mechanisms in Bipolar Membranes. ACS Appl. Mater. Interfaces 2020, 12, 52509-52526.
- (38) Volgin, V. M.; Davydov, A. D. Ionic transport through ionexchange and bipolar membranes. J. Membr. Sci. 2005, 259, 110-121.
- (39) Hibbs, M. R.; Hickner, M. A.; Alam, T. M.; McIntyre, S. K.; Fujimoto, C. H.; Cornelius, C. J. Transport properties of hydroxide and proton conducting membranes. Chem. Mater. 2008, 20, 2566-2573
- (40) Zhang, C. Y.; He, D.; Ma, J. X.; Tang, W. W.; Waite, T. D. Faradaic reactions in capacitive deionization (CDI)—problems and possibilities: A review. Water Res. 2018, 128, 314-330.
- (41) Landon, J.; Gao, X.; Omosebi, A.; Liu, K. L. Emerging investigator series: local pH effects on carbon oxidation in capacitive deionization architectures. Environ. Sci.: Water Res. Technol. 2021, 7, 861-869.
- (42) Dykstra, J. E.; Keesman, K. J.; Biesheuvel, P. M.; van der Wal, A. Theory of pH changes in water desalination by capacitive deionization. Water Res. 2017, 119, 178-186.
- (43) Nagasawa, H.; Iizuka, A.; Yamasaki, A.; Yanagisawa, Y. Utilization of Bipolar Membrane Electrodialysis for the Removal of Boron from Aqueous Solution. Ind. Eng. Chem. Res. 2011, 50, 6325-6330.

# **□** Recommended by ACS

**Precise Cation Separations with Composite Cation-Exchange Membranes: Role of Base Layer Properties** 

Ryan M. DuChanois, Menachem Elimelech, et al.

APRII 06 2023

**ENVIRONMENTAL SCIENCE & TECHNOLOGY** 

READ 2

**Enhancing the Total Salt Adsorption Capacity and Monovalent Ion Selectivity in Capacitive Deionization Using** a Dual-Layer Membrane Coating Electrode

Chengyi Wang, Jiahui Shao, et al.

DECEMBER 05, 2022

ACS ES&T WATER

READ M

Influences of Divalent Ions in Natural Seawater/River Water on Nanofluidic Osmotic Energy Generation

Fenhong Song, Yinghua Qiu, et al.

OCTOBER 16, 2022

LANGMUIR

RFAD 17

#### Bipolar Membrane Capacitive Deionization for pH-Assisted **Ionic Separations**

Tanmay Kulkarni, Christopher G. Arges, et al.

MAY 10, 2023

ACS ES&T ENGINEERING

READ **C** 

Get More Suggestions >